ACS APPLIED MATERIALS & INTERFACES

Research Article

www.acsami.org

Stimulus-Responsive, Biodegradable, Biocompatible, Covalently Cross-Linked Hydrogel Based on Dextrin and Poly(*N*-isopropylacrylamide) for in Vitro/in Vivo Controlled Drug Release

Dipankar Das,[†] Paulomi Ghosh,[‡] Animesh Ghosh,[§] Chanchal Haldar,[†] Santanu Dhara,[‡] Asit Baran Panda,[∥] and Sagar Pal*[,†]

[†]Polymer Chemistry Laboratory, Department of Applied Chemistry, Indian School of Mines, Dhanbad 826004, India

[‡]Biomaterials and Tissue Engineering Laboratory, School of Medical Science & Technology, Indian Institute of Technology, Kharagpur 721302, India

[§]Departmental of Pharmaceutical Sciences, Birla Institutes of Technology, Mesra, Ranchi, Jharkhand 835215, India

[∥]Discipline of Inorganic Materials and Catalysis, Central Salt and Marine Chemicals Research Institute (CSIR), Bhavnagar, Gujarat 364002, India

Supporting Information

ABSTRACT: A novel stimulus-sensitive covalently cross-linked hydrogel derived from dextrin, *N*-isopropylacrylamide, and *N*,*N*′-methylene bis(acrylamide) (c-Dxt/pNIPAm), has been synthesized via Michael type addition reaction for controlled drug release application. The chemical structure of c-Dxt/pNIPAm has been confirmed through Fourier transform infrared (FTIR) spectroscopy and ^{1}H and ^{13}C NMR spectral analyses. The surface morphology of the hydrogel has been studied by field emission scanning electron microscopic (FE-SEM) and environmental scanning electron microscopic (E-SEM) analyses. The stimulus responsiveness of the hydrogel was studied through equilibrium swelling in various pH media at 25 and 37 °C. Rheological study was performed to measure the gel strength and gelation time. Noncytotoxicity of c-Dxt/pNIPAm hydrogel has been studied using human mesenchymal stem cells (hMSCs). The biodegradability of c-Dxt/pNIPAm was confirmed using hen egg lysozyme. The in vitro and in vivo release studies of ornidazole and ciprofloxacin imply that c-Dxt/pNIPAm delivers both drugs in a controlled way and would be an excellent alternative for a dual drug carrier. The FTIR, powder X-ray diffraction (XRD), and UV−vis−near infrared (NIR) spectra along with the computational study predict that the drugs remain in the matrix through physical interaction. A stability study signifies that the drugs (ornidazole ∼97% and ciprofloxacin ∼98%) are stable in the tablet formulations for up to 3 months.

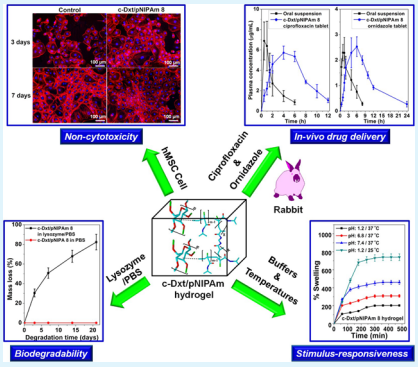

KEYWORDS: *biodegradable, noncytotoxicity, controlled drug release, dextrin, hydrogel*

1. INTRODUCTION

In drug delivery applications, the oral route is the most suitable mode for delivering drugs safely, to improve the curative effect of the drugs.[1,2] Controlled drug delivery matrix via oral route administration should prevent the attack of enzymes as well as the effect of pH gradients for gastrointestinal transit time (3−16 h) from mouth to cecum.[1] Consequently, resistance to acidic pH and enzyme along with sustained release profiles are essential features for a promising oral drug delivery matrix in a controlled release system.[1,2] In recent times, controlled drug delivery systems are developed to address the drawbacks of the conventional drug delivery systems by enhancing drug solubility, sustaining release time, reducing side effects, and so on.[3−5] Several drug delivery systems such as particulate carriers,[6,7] polymeric gels,[8,9] and lipids[10,11] have been used as drug delivery matrixes. At the present time, stimuli-sensitive chemically cross-linked hydrogels demonstrate excellent potential as controlled drug release matrixes. The release behaviors of drugs can easily be controlled with surrounding properties, such as pH,[12,13] temperature,[14] light,[15] and electric field.[16] Out of these hydrogels, pH-/temperature-sensitive hydrogels are widely used in biomedical applications as these factors can be controlled and are pertinent for both in vitro and in vivo conditions.[1,17−19]

Hydrogels are the hydrophilic, cross-linked polymeric networks that exhibit the ability to swell in aqueous medium or in biomedical fluids, without dissolving, and retain a large amount of water within their three-dimensional structure.[12,13] The biocompatible nature of a hydrogel is attributed to its capability to simulate the neighboring tissue owing to its high

Received: April 6, 2015
Accepted: June 12, 2015
Published: June 12, 2015

DOI: 10.1021/acsami.5b02975
ACS Appl. Mater. Interfaces 2015, 7, 14338−14351

Table 1. Synthesis Details and Percent CR and Percent ESR of the c-Dxt/pNIPAm Hydrogels, with 0.0031 mol of Dextrin

hydrogelator	initiator concn (mol × 10^{-5})	cross-linker concn (mol × 10^{-3})	monomer concn (mol × 10^{-4})	% CR	% ESR			
					pH 1.2, 37 °C	pH 6.8, 37 °C	pH 7.4, 37 °C	pH 7.4, 25 °C
c-Dxt/pNIPAm 1	0.92	3.08	2.20	75.50	387 ± 19	522 ± 26	748 ± 17	1248 ± 32
c-Dxt/pNIPAm 2	1.85	3.08	2.20	78.25	320 ± 16	452 ± 22	638 ± 19	988 ± 29
c-Dxt/pNIPAm 3	3.69	3.08	2.20	47.65	353 ± 17	493 ± 24	684 ± 21	1084 ± 34
c-Dxt/pNIPAm 4	1.85	0.77	2.20	82.57	458 ± 22	608 ± 30	924 ± 26	1524 ± 46
c-Dxt/pNIPAm 5	1.85	1.54	2.20	81.37	241 ± 12	347 ± 17	497 ± 20	777 ± 23
c-Dxt/pNIPAm 6	1.85	4.62	2.20	80.60	279 ± 13	387 ± 19	537 ± 22	827 ± 21
c-Dxt/pNIPAm 7	1.85	1.54	1.10	82.50	304 ± 15	407 ± 20	582 ± 23	862 ± 23
c-Dxt/pNIPAm 8	1.85	1.54	3.31	84.90	203 ± 10	309 ± 15	459 ± 18	739 ± 21
c-Dxt/pNIPAm 9	1.85	1.54	3.86	73.16	427 ± 22	567 ± 28	849 ± 22	1399 ± 29

water content.[20,21] Hydrogels are capable of potential biotechnological applications that employ their swelling and deswelling dynamics.[22] Because of these characteristics, hydrogels have widely been used in various biomedical fields including controlled drug delivery,[12,13,23] tissue engineering, and regenerative medicine,[24,25] and also as diagnostic biomedical biosensors.[26] However, the quantity and homogeneous distribution of drug molecules in hydrogel based device systems are vital for practical applications, which are the major disadvantages of the present loading matrixes and injected delivery systems.[12] Besides, the higher swelling capacity of the hydrogel results in rapid drug release within a few hours to several hours. Consequently, the efficacy of the drug delivery system is reduced and often causes multiple harmful side effects.[27,28]

In recent years most of the reports[29] are focused on mechanical properties,[30,31] swelling properties,[32] and stimulus sensitivity[30,32] of the hydrogels; while biocompatible, biodegradable, and prolonged oral drug delivery matrixes such as tablet formulations are still less studied. Therefore, it is imperative to develop the materials which would be biocompatible and biodegradable, and they should have controlled swelling nature and minimum erosion rate. Besides, the material should deliver the drugs in a sustained way.

Recently, biopolymer based chemically cross-linked hydrogels have been used as drug carriers.[12,13] Dextrin is a natural polysaccharide with immense prospects for the development of hydrogels owing to its demonstrated medical acceptability and proficient absorption because of degradation through amylases.[33,34] Poly(*N*-isopropylacrylamide) (pNIPAm) is thermoresponsive due to its lower critical solution temperature (LCST) between 30 and 32 °C,[1] while the human body temperature is ∼37 °C.[1,35,36] This thermosensitive polymer has been used for the development of gels[37] and beads,[38] as a drug carrier,[12] for bioactive molecule separations,[39] and for catalysts.[40] The copolymer of NIPAm with other functional monomers has been used in various fields.[41] Besides, in the presence of heat and initiator, *N*,*N*′-methylene bis(acrylamide) (MBA) can easily form a three-dimensional network owing to its four reactive sites (two double bonds) and thus would be suitable as a cross-linker for the development of hydrogels.[12,13]

With the advantages of synthetic polymers as well as natural biopolymers, a stimulus-responsive (pH and temperature) covalently cross-linked hydrogel has been synthesized using dextrin (Dxt) as biopolymer, NIPAm as monomer, MBA as cross-linker, and potassium persulfate (KPS) as initiator. Because of the covalent attachment of cross-linker (MBA), the hydrogel (c-Dxt/pNIPAm) showed excellent controlled swelling characteristics as well as minimum erosion rate, which have significant effect on control release behavior. Besides, c-Dxt/pNIPAm displayed noncytotoxicity and a biodegradable nature that are major concerns for the drug delivery application. Further, both in vitro and in vivo release profiles demonstrated sustain release behavior of ornidazole and ciprofloxacin from the c-Dxt/pNIPAm hydrogel. Drug stability study suggested that both tablet formulations are comparatively stable (ornidazole ∼97% and ciprofloxacin ∼98%) up to 3 months of study periods.

For the first time, a covalently cross-linked hydrogel based on dextrin and NIPAm (c-Dxt/pNIPAm) has been employed as controlled release matrix for ornidazole and ciprofloxacin delivery. Therefore, the improbable characteristics of the synthesized cross-linked hydrogel, such as stimulus responsiveness, controlled swelling property, noncytotoxicity, biodegradability, and in vitro/in vivo sustained release behavior of both drugs (ornidazole and ciprofloxacin) in tablet formulations can solve the problems of loading systems and injected delivery systems and thus would be a new platform for controlled release of ornidazole and ciprofloxacin.

2. EXPERIMENTAL SECTION

2.1. Chemicals. Dextrin (from Fluka, Switzerland), *N*-isopropylacrylamide (from Acros Organics, New Jersey, USA), *N*,*N*′-methylene bis acrylamide (MBA) (from Loba Chemie Pvt. Ltd., Mumbai, India), potassium persulfate (KPS) (from Glaxo Smith Kline Pharmaceuticals Ltd., Mumbai, India), acetone (from E-Merck (I) Pvt. Ltd., Mumbai, India), ornidazole (from Endoc Pharma, Rajkot, Gujarat, India), ciprofloxacin (from Sigma-Aldrich, Germany), guar gum (from Hindustan Gum and Chemicals Ltd., Haryana, India), and egg white lysozyme hydrochloride (from TCI Pvt. Ltd., Tokyo, Japan) were used as received. Double distilled water (DW) was used for experimental works.

2.2. Synthesis. *Preparation of c-Dxt/pNIPAm Hydrogelator.* The synthesis of cross-linked hydrogelator based on dextrin and poly(*N*-isopropylacrylamide) in the presence of cross-linker and initiator proceeds through free radical polymerization as follows:

First, 0.0031 mol of dextrin was dissolved in 25 mL of distilled water in a three-necked RB flask. The flask was fitted with a magnetic stirrer along with oil bath (temperature of the oil bath was maintained at 50 °C and the stirring speed was fixed at 400 rpm). Afterward, nitrogen gas was purged to create an inert atmosphere and the reaction temperature was raised to 75 °C. After 15 min, an aqueous solution of KPS (Table 1) was added to the dextrin solution. After 10 min, the required amount of aqueous solution of *N*-isopropylacrylamide (Table 1) was added. When the solution became milky white, cross-linker (MBA) (Table 1) dissolved in 5 mL of water was added to this solution and stirring was continued at 75 °C and 400 rpm for a further 6 h. After that, the reaction mixture was cooled and the hydrogelator was precipitated in acetone to remove the homopolymer and excess

DOI: 10.1021/acsami.5b02975
ACS Appl. Mater. Interfaces 2015, 7, 14338−14351

amount of cross-linker. Finally, the product was dried in vacuum oven (at 35 °C) until a constant weight of the hydrogelator was achieved. The synthesis parameters are reported in Table 1. The dried hydrogelator, i.e., c-Dxt/pNIPAm xerogel, was used for characterizations and drug delivery application.

2.3. Characterization. Fourier transform infrared (FTIR) spectra of dextrin, c-Dxt/pNIPAm 8 xerogel, ornidazole/ciprofloxacin drugs, and triturated form of corresponding tablets were recorded using the KBr pellet method (Model IR-PerkinElmer, Spectrum 2000) within the scan range 400−4000 cm^{-1}.

^1H NMR spectra of dextrin, NIPAm, MBA, and c-Dxt/pNIPAm 8 hydrogelator (in DMSO-d_6) were recorded at 400 MHz on a Bruker spectrophotometer, and solid state ^{13}C NMR spectra of dextrin and the cross-linked xerogel were recorded at 500 MHz on a Bruker Avance II-500NMR spectrophotometer.

Thermogravimetric analysis (TGA) was performed using a TGA analyzer (Model STA449F3, Netzsch, Germany) in an inert atmosphere of N_2. The heating rate was 5 °C/min.

The surface morphology of dextrin and microstructure of c-Dxt/pNIPAm 8 xerogel were analyzed using field emission scanning electron microscopy (FE-SEM Supra 55, Zeiss, Germany). The surface morphology of swollen c-Dxt/pNIPAm 8 hydrogelator (in phosphate buffered saline, pH 7.4 (PBS 7.4) was investigated by environmental scanning electron microscopy (E-SEM, Model EVO 18, Zeiss, Germany).

Powder X-ray diffraction (XRD) spectra of c-Dxt/pNIPAm 8 xerogel, ornidazole, ciprofloxacin, and the powder form of corresponding tablets were recorded using a Bruker X-ray diffractometer (Bruker, D8-Fecus, Germany).

Solid state UV−visible−near infrared (NIR) studies of c-Dxt/pNIPAm 8 xerogel, drugs, and corresponding tablets were performed using a Cary series UV−vis-NIR spectrophotometer (Cary −5000).

2.4. Rheological Characteristics. *Gel Kinetics.* The gelation kinetics of c-Dxt/pNIPAm 8 was determined by measuring the dynamic time sweep (0−20 min) and the dynamic frequency sweep (0.1−3.0 Hz) at various cure times with parallel plate geometry at the reaction temperature, i.e., 75 °C. Besides, the rheological features of c-Dxt/pNIPAm 8 hydrogelator were investigated at the gel state (after equilibrium swelling was reached in PBS 7.4) at a temperature of 37 ± 0.1 °C (using a Bohlin Gemini-2 rheometer, Malvern, U.K.). The experimental procedure has been explained in detail in the Supporting Information.

2.5. Biodegradation Study. An enzymatic biodegradation test of c-Dxt/pNIPAm 8 xerogel film was carried out using lysozyme from egg white as described in the literature.[42−45] Briefly, the preweighed c-Dxt/pNIPAm 8 xerogel films (10 × 10 × 0.1 mm^3) were immersed in lysozyme solution (pH 7) at a natural concentration as observed within the human body (1.5 μg/mL). The temperature of the lysozyme solution was maintained at 37 °C. The solution was refreshed daily to make continuous enzyme activity.[42] After 3, 7, 14, and 21 days, the films were withdrawn from the solution, washed with double distilled water, and dried in a vacuum oven for 72 h. Afterward, they were reweighed. The degree of in vitro degradation has been expressed as percent weight loss of the dried films vs time.[45] Another film, dispersed in phosphate buffer (pH 7) without lysozyme, was also studied for weight loss for comparison.

2.6. In Vitro Cytotoxicity Studies. Equal weights of powdered c-Dxt/pNIPAm 8 xerogel were used for pellets. The pellets were kept in 24 well plates for in vitro cytotoxicity studies. The in vitro cytotoxicity study has been explained in detail in the Supporting Information.

Cell Proliferation. DNA quantification assay of hMSCs grown on lysine coated coverslips placed in 24 well plates and c-Dxt/pNIPAm 8 hydrogel pellet was performed with Hoechst 33258 (Invitrogen) as per the manufacturer's instructions. Fluorescence was recorded using a fluorescence spectrophotometer. The DNA standard curve was acquired from a known number of cells.[46] The morphology of the adherent cells was examined using fluorescent imaging. For fluorescent imaging, cells at the third day were fixed with 3.7% paraformaldehyde, subsequently washed repeatedly with PBS, and permeabilized using Triton-X (Sigma), and unspecific sites were blocked with bovine serum albumin (BSA, Merck, India).[46] Actin filaments and nuclei of cells were stained with rhodamine phalloidin (Molecular Probes) and 4′,6-diamidino-2-phenylindole, dihydrochloride (DAPI; Molecular Probes), and imaged in a Zeiss Axiovision (Germany) microscope. For repeatability, the experiment was executed in triplicate. Results are represented as mean ± standard deviation (SD). Statistical analysis was carried out through one-way ANOVA followed by Tukey post hoc analysis in Origin Pro 8 software. Significance was determined at $p < 0.05$.

2.7. Stimulus-Responsive Swelling Characteristics and Its Kinetics. The swelling characteristics of c-Dxt/pNIPAm hydrogelator were performed by assessing the equilibrium swelling ratio (ESR) at various pHs (1.2, 6.8, and 7.4) as well as at different temperatures (25 and 37 °C at a constant pH 7.4). The details of swelling study have been given in the Supporting Information. Also, the rate of swelling was measured using the Voigt model (see Supporting Information).[12,44]

2.8. In Vitro Ornidazole and Ciprofloxacin Release Studies. *Preparation of Tablets.* The ornidazole and ciprofloxacin tablets were prepared for in vitro release study using the following composition of xerogel (matrix):ciprofloxacin/ornidazole (drug):guar gum (binder) = 450 mg:500 mg:50 mg. The detailed procedure for the preparation of tablets has been given in the Supporting Information.

Estimation of Drug Release from c-Dxt/pNIPAm. The in vitro release of entrapped ornidazole/ciprofloxacin drugs from c-Dxt/pNIPAm 8 based tablet formulation was examined using a dissolution apparatus (Lab India, Model DS 8000). The release study was performed with a rotation of 60 rpm at 25 ± 0.5 °C and 37 ± 0.5 °C. The release study was executed with 900 mL of simulated gastric fluid (SGF, pH 1.2) for 2 h, with phosphate buffer (pH 6.8) for the next 3 h (for the colonic drug ornidazole), and after that with simulated intestinal fluid (SIF, pH 7.4) up to 24 h. The percent cumulative drug release was measured using a UV−visible spectrophotometer (Shimadzu, Japan; Model UV 1800). The drug release kinetics and mechanism were determined by fitting the release data to various mathematical models. The details of various kinetics models have been explained in the Supporting Information.

Determination of Percent Erosion of Tablets. During drug release from dextrin and c-Dxt/pNIPAm hydrogel systems, erosion took place after attainment of the "critical gel concentration" of the hydrogel. The determination of percent erosion has been stated in the Supporting Information.

2.9. Stability Study of Drugs in Tablet. To observe the environmental effect on tablet formulation, a stability study was performed for up to 3 months in the same way as reported earlier.[12,23,44] The detailed procedure has been explained in the Supporting Information.

2.10. Computational Study for Determining the Drug−Matrix Interaction. All the electronic structure optimizations and visualizations were performed with the help of a personal computer (PC) using Gaussian 09[47] and GaussView 5.0[48] program package. Besides, the calculations were performed with density functional theory using the Becke three-parameter Lee−Yang−Parr (B3LYP) procedure.[49−51]

Recently, it has been established that B3LYP is a reliable method for accounting of charged strong halogen bonds.[52] Vibrational frequencies were calculated at the same level of theory to ensure that the structures are real minima on the potential energy surface.[53] All the calculations were performed in the gaseous state without any symmetry constrain. To reduce the excess computational load, a single monomeric unit of the c-Dxt/pNIPAm hydrogelator was considered as a representation of the whole c-Dxt/pNIPAm hydrogelator unit. The c-Dxt/pNIPAm hydrogelator was synthesized by cross-linking poly(*N*-isopropylacrylamide) (pNIPAm) on dextrin moiety in the presence of MBA cross-linker. It was assumed that the grafting of pNIPAm in the dextrin backbone can be through primary or secondary alcoholic groups present in the dextrin molecule. We have considered both possibilities, i.e., pNIPAm grafted on dextrin backbone via primary and secondary alcoholic groups, and tried to establish their affinity toward the drugs (ornidazole and ciprofloxacin). The interaction energy (E_{int}) was

DOI: 10.1021/acsami.5b02975
ACS Appl. Mater. Interfaces 2015, 7, 14338−14351

Scheme 1. Probable Reaction Mechanism for Synthesis of c-Dxt/pNIPAm Hydrogelator

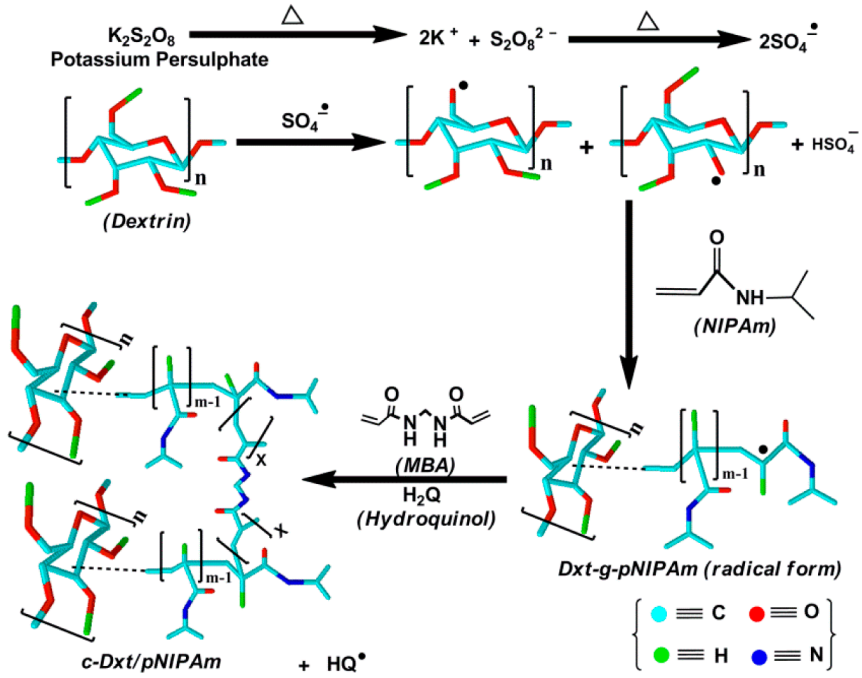

calculated from the difference of total energy of the c-Dxt/pNIPAm@ drugs and the total energy of optimized geometry of the c-Dxt/pNIPAm hydrogelator and drugs.

2.11. In Vivo Pharmacokinetic Study. *Estimation of Ciprofloxacin in Rabbit Plasma.* Ciprofloxacin contained in rabbit plasma from oral suspension and in tablet dosage form was measured by HPLC (Knaur, Germany). Gemifloxacin was used as an internal standard. Analysis was performed by a NOVAPAC C18 (Waters, USA) column (150 mm × 4.6 mm, particle size 3 μm) using an isocratic elution mode with a mobile phase of 25 mM phosphoric acid:acetonitrile (83:17 v/v). The pH was kept at 3.0 using phosphoric acid at a flow rate of 1 mL/min at 276 nm using a UV/vis detector. The total run was stabilized up to 30 min. Data acquisition was performed using EuroChrom software. The plasma calibration curve was prepared in the range 0.5−20 μg/mL. Liquid−liquid extraction (extractive solvent was dichloromethane) technique was adopted for the extraction of analytes from the biological matrix.[54]

Estimation of Ornidazole in Rabbit Plasma. Ornidazole concentration in rabbit plasma was determined by HPLC (Knaur, Germany) as per the reported method described by Sahoo et al.[54] with slight modification. Ranitidine was used as an internal standard. Analysis was investigated at room temperature using a Cyano column (250 mm × 4.6 mm, particle size 5 μm) under isocratic elution mode with a mobile phase of 10 mM dipotassium hydrogen phosphate buffer (pH 4.8):acetonitrile (50:50 v/v) with a flow rate of 1 mL/min at 320 nm using a UV/vis detector. The plasma calibration curve was prepared in the range 0.1−10 μg/mL.[54]

Animal Housing and Handling. Albino rabbits, 2.5−3 kg, three per group, were used in the study in accordance with the protocol approved by the Institutional Animal Ethical Committee (CPCSEA Approval No. 621/02/ac/CPCSEA) at the Department of Pharmaceutical Sciences, Birla Institute of Technology, Mesra, Ranchi, India. All rabbits were housed individually in polycarbonate cages with sufficient food and water at 20−25 °C and 40−70% relative humidity in a 12 h light−dark cycle.[55] The oral suspension and tablet dosage form were directed after 12 h of fasting.[54,55]

Pharmacokinetic Analysis. Pharmacokinetic studies of ciprofloxacin and ornidazole were conducted on white albino rabbits. The detailed study has been explained in the Supporting Information. The pharmacokinetic parameters were determined using zero moment noncompartmental pharmacokinetic modeling.[54,55]

3. RESULTS AND DISCUSSION

3.1. Synthesis of c-Dxt/pNIPAm Hydrogelator. The c-Dxt/pNIPAm hydrogelator was synthesized through free radical polymerization technique. It is presumed that the initiator creates free radical sites on dextrin, which reacts with poly(*N*-isopropylacrylamide) to form the copolymer. Afterward, because of the presence of two double bonds in MBA, it forms four reactive sites that would be able to link with two copolymer moieties to form a three-dimensional (3-D) network as proposed in Scheme 1. The effect of reaction parameters was studied by developing series of hydrogels (Table 1).

Effect of Reaction Parameters. With variation of initiator concentration (0.92×10^{-5}−3.69×10^{-5} mol, see Table 1), it was observed that c-Dxt/pNIPAm 2 demonstrates lower percent equilibrium swelling ratio (% ESR), i.e., higher percent cross-linking ratio (% CR). This is because of the fact that, at comparatively higher initiator concentrations, the maximum number of free radical sites would be created on dextrin along with on the grafted network that could be cross-linked with MBA, resulting in higher % CR. Besides, with alteration of the cross-linker concentration (0.77×10^{-3}−4.62×10^{-3} mol, Table 1), maximum % CR was observed with MBA concentration of 6.48×10^{-3} mol. This is due to the fact that % CR would be higher with incorporation of a more amount of cross-linker in the hydrogel structure. This results in the formation of a more dense and rigid structure, ensuring less % ESR. The monomer concentration (i.e., pNIPAm) was also varied from 1.10×10^{-4} to 3.86×10^{-4} mol. It was found that, at relatively higher monomer concentration, the % ESR increased, i.e., % CR is less (Table 1), which is mainly due to the formation of homopolymer with higher monomer concentration. The optimized hydrogelator was considered on the basis of higher % CR and lower % ESR.

3.2. Characterization. In the FTIR spectrum of *N*-isopropylacrylamide (Figure S1a, Supporting Information), two strong absorption peaks at 3294 and 2974 cm^{-1} are assigned to the secondary N−H and C−H stretching

DOI: 10.1021/acsami.5b02975
ACS Appl. Mater. Interfaces 2015, 7, 14338−14351

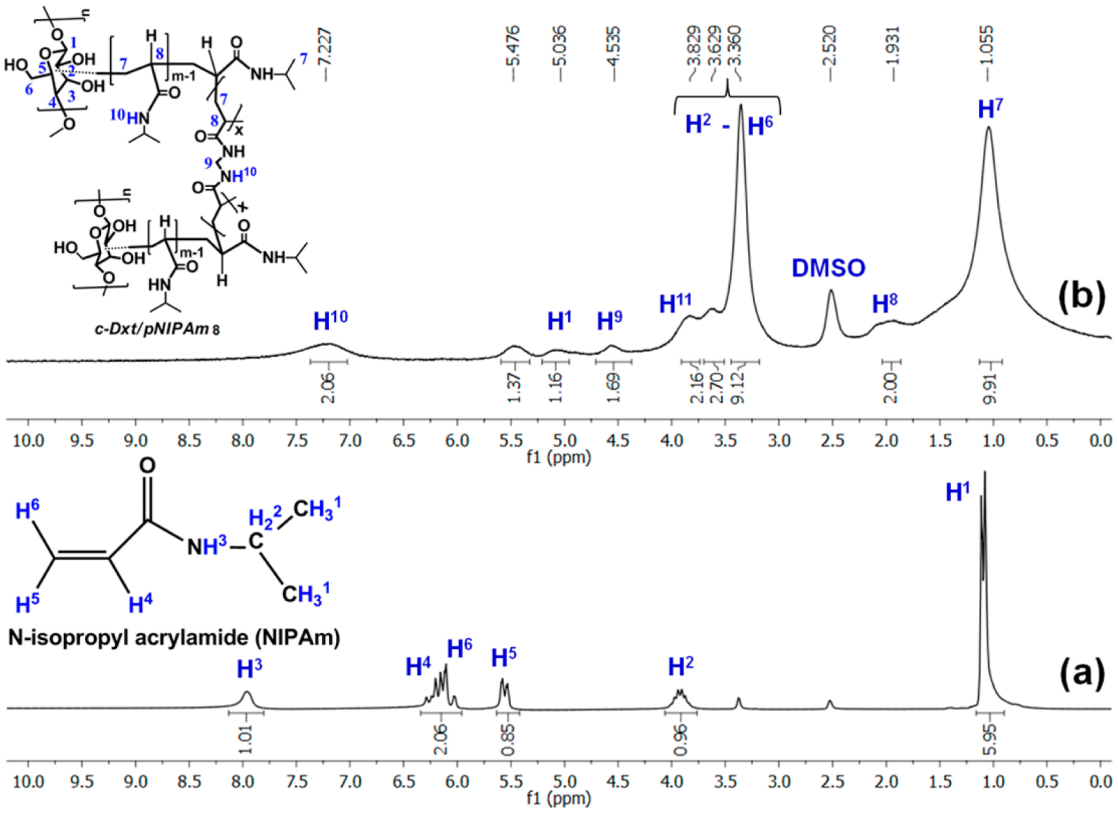

Figure 1. ^{1}H NMR spectra of (a) NIPAm and (b) c-Dxt/pNIPAm 8 hydrogelator in DMSO-d_6.

vibrations, respectively. The peaks at 1650 and 1550 cm^{-1} are attributed to amide I and amide II bands. The peaks at 1614 and 1243 cm^{-1} are due to C═C bond vibration and C−N stretching frequency. In the FTIR spectrum of the synthesized hydrogelator [c-Dxt/pNIPAm 8] (Figure S1b, Supporting Information), the O−H of dextrin,[23] the N−H of MBA and pNIPAm overlap, leading to a broad peak at 3439 cm^{-1}. The peak at 2928 cm^{-1} is due to C−H stretching of the −CH$_3$ group, which originates from poly(NIPAm) present on the dextrin moiety. Three peaks at 1661, 1561, and 1267 cm^{-1} are attributed to the stretching frequencies of amide I, amide II, and C−N bond, respectively. These three peaks suggest the presence of cross-linker (MBA) in addition to NIPAm in the cross-linked network. The peaks at 1161 and 1028 cm^{-1} are characteristic peaks of C−O−C stretching vibrations of dextrin. The intense peak of NIPAm at 1614 cm^{-1} is absent in the FTIR spectrum of c-Dxt/pNIPAm 8, suggesting the polymerization of *N*-isopropylacrylamide and cross-linking of MBA. The FTIR spectrum of ornidazole[12] demonstrates that peaks at 3314, 1365, and 745 cm^{-1} are due to −O−H stretching vibrations, the symmetric stretching mode of the NO$_2$ group, and the stretching frequency of the C−Cl bond, respectively.[12] In the spectrum of triturated form of ornidazole tablet (Figure S1c, Supporting Information), the amide I stretching frequency shifted from 1661 to 1650 cm^{-1}, amide II shifted from 1561 to 1539 cm^{-1}, the N−O stretching frequency shifted from 1372 to 1357 cm^{-1}, C−Cl shifted from 745 to 728 cm^{-1}, and −O−H/N−H stretching frequency shifted from 3439 to 3324 cm^{-1}, which suggest that probably H-bonding interactions are present between the hydrogelator and drugs as shown in Figure S2 in the Supporting Information. In the FTIR spectrum of ciprofloxacin,[23] the characteristic peaks at 3528, 1713, 1626, and 1042 cm^{-1} are attributed to stretching vibrations of O−H and the carbonyl (C═O) group, N−H bending of the quinolone ring, and the stretching frequency of the C−F group, respectively.[23] The FTIR spectrum of ciprofloxacin tablet (Figure S1d, Supporting Information) indicates that the stretching frequency of carbonyl groups shifted from 1713 to 1694 cm^{-1}, amide I shifted from 1661 to 1617 cm^{-1}, amide II shifted from 1561 to 1490 cm^{-1}, and the C−F bond stretching frequency moved from 1042 to 1028 cm^{-1}, suggesting that drugs remain in the c-Dxt/pNIPAm matrix by physical interaction as shown in Figure S2 in the Supporting Information.

NMR Spectra. The ^{1}H NMR spectrum of dextrin[44] (400 MHz, DMSO-d_6) showed the characteristic peaks in δ = 3.323−4.450 ppm due to the presence of various protons of the polysaccharide ring. The peaks between δ = 4.962−5.061 ppm and δ = 5.362−5.449 ppm correspond to the anomeric protons. Again, peaks between δ = 2.996−3.042 ppm and δ = 2.861−2.926 ppm indicate the presence of protons for primary −OH and secondary −OH groups, respectively.[44]

The ^{1}H NMR spectrum of *N*-isopropylacrylamide (Figure 1a and Figure S3, Supporting Information, 400 MHz, DMSO-d_6, ppm) showed δ = 7.968 (broad, s, 1H, i.e., for H^3), 6.021−6.288 (m, 2H, i.e., for H^4 and H^6), 5.530−5.590 (m, 1H, i.e., for H^5), 3.841−3.976 (m, 2H, i.e., for H^2), and 1.080−1.113(t, 6H, i.e., for H^1).

The ^{1}H NMR spectrum of MBA[44] (400 MHz, DMSO-d_6) showed the characteristic peaks at δ = 8.744, 6.226−6.358, 6.099−6.199, and 4.549−4.608 ppm for amide proton, three sp^2 hybridized protons, and methylene protons, respectively.[44]

The polymerization of NIPAm and the cross-linking reaction was confirmed by investigating the NMR spectra of the reactant and products. The intensity of the corresponding chemical

DOI: 10.1021/acsami.5b02975
ACS Appl. Mater. Interfaces 2015, 7, 14338−14351

shifts of MBA in the hydrogel structure was used to calculate the cross-linking density of c-Dxt/pNIPAm 8 hydrogelator.[56]

For the ^{1}H NMR spectrum of c-Dxt/pNIPAm 8 hydrogelator (Figure 1b, 400 MHz, DMSO-d_6), the protons in the hydrogelator and their corresponding ^{1}H NMR signals are represented as H^8 for −CH− at the chemical shift δ = 1.931 ppm for poly(NIPAm) and MBA. The peak at δ = 1.055 ppm is H^7 for $-CH_2/-CH_3$ of poly(NIPAm) and $-CH_2$ of MBA molecules. The peaks at δ = 3.360−3.829, 5.036, and 5.476 ppm suggest the presence of dextrin in the hydrogelator, i.e., for H^1 and H^2 to H^6 protons (Figure 1b). The peak at δ = 7.227 ppm for −NH groups of poly(NIPAm)/MBA, i.e., for H^{10} protons, and the peak at δ = 3.829 ppm indicate the presence of isopropylene hydrogen (H^{11}), which arises from NIPAm (Figure 1b).

Again, the peak at δ = 4.535 ppm is due to the methylene protons of MBA, i.e., for H^9 protons. The absence of peaks in δ = 2.861−3.042 ppm confirm the reactivity of −OH groups of dextrin toward poly(NIPAm). The peaks at 7.227 and 1.055 ppm confirm the presence of NIPAm moiety in the hydrogelator (Figure 1b). On the other hand, the peaks at 7.227 and 4.535 ppm suggest the incorporation of MBA molecule into the network structure. Besides, the disappearance of peaks in δ = 5.530−6.358 ppm for vinylic protons and the appearance of the peaks at δ = 1.055−1.931 ppm indicate the polymerization of both NIPAm and MBA moieties during the formation of c-Dxt/pNIPAm hydrogelator. This also supports that polymerization and cross-linking process indeed took place in c-Dxt/PNIPAm 8. Thus, the ^{1}H NMR spectra confirmed the successful synthesis of c-Dxt/pNIPAm hydrogelator.

Determination of Cross-Linking Density in c-Dxt/pNIPAm 8 Hydrogelator. The cross-linking density of c-Dxt/pNIPAm 8 hydrogelator was determined[56] with the help of peak intensity of sp^3 carbon protons formed from sp^2 carbon protons during polymerization and cross-linking reactions (i.e., H^7 and H^8) and methylene protons of the cross-linker (i.e., H^9) (see Figure 1b). The H^7 peak intensity, i.e., I_{H^7}, is comparative to the number of H^7 protons, while the peak intensity of H^8, i.e., I_{H^8}, is relative to the number of H^8 protons. Thus, the peak at δ = 1.055 exists for $-CH_2/-CH_3$ of poly(NIPAm) and $-CH_2$ of MBA molecules in the hydrogelator, i.e., for H^7. However, the ^{1}H NMR spectrum of *N*-isopropylacrylamide provides the peaks at δ =1.080−1.113 ppm for 6H of $-CH_3$ groups. Thus, the deduction value between these two peak intensities provides the peak intensity of $-CH_2$ protons of both pNIPAm and MBA formed during polymerization and cross-linking reactions. Therefore, both $-CH_2$ groups of pNIPAm and MBA have equal intensity. Here m and X represent the repeating units of pNIPAm and MBA. Subsequently, the degree of cross-linking would be $X/(m + X)$. Again, both $I_{(-CH_2-)}$ and $I_{(-CH-)}$ would be directly proportional to $m + X$. Moreover, it was obvious from Figure 1b that the peak area of $-CH_2-$ is double the peak area of −CH−. It has been assumed that $I_{H^8} = 2$ for two −CH− groups. This has been used as a basis to determine the intensity of peak H^9, which expresses the amount of MBA in the hydrogelator or the degree of cross-linking. The cross-linking density was measured using eq 1.[56]

$$\text{cross-linking density (CD)} = \frac{X}{m + X} = \frac{I_{H^9}}{I_{(-CH_2-)}} \quad (1)$$

Here, we have evaluated the cross-linking density (CD) of c-Dxt/pNIPAm 8 using eq 1 and it was found to be ∼42.68% (having I_{H^9} = 1.69, $I_{(-CH_2-)}$ = 9.91 − 5.95 = 3.96 (see Table S1, Supporting Information).

The ^{13}C NMR spectrum (in solid state) of c-Dxt/pNIPAm 8 xerogel is shown in Figure 2. Dextrin demonstrates four

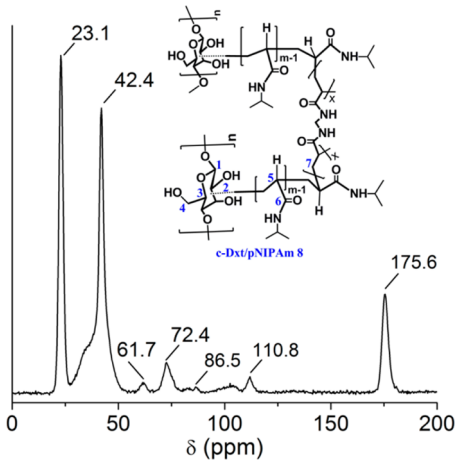

Figure 2. Solid state ^{13}C NMR spectrum of c-Dxt/pNIPAm 8 xerogel.

characteristics peaks at δ = 111.4, 88.5, 79.4, and 68.1 ppm.[12] In contrast to dextrin, the c-Dxt/pNIPAm 8 xerogel has few extra peaks. The peak at 175.6 ppm is because of the carbon atoms of amide groups for NIPAm and MBA moiety (Figure 2). Peaks at 42.4 and 23.1 ppm are due to carbon atom $-CH_3$ and −CH− groups of NIPAm along with the sp^3 carbon formed during the polymerization of NIPAm and cross-linker (see Scheme 1) (i.e., during polymerization, two sp^2 hybridized carbon atoms of pNIPAm and MBA converted to sp^3 hybridized carbon atoms). Thus, from ^{1}H and ^{13}C NMR spectral analysis, it is evident that pNIPAm has been cross-linked successfully on the dextrin moiety.

The thermogram of c-Dxt/pNIPAm 8 xerogel (Figure S4, Supporting Information) demonstrates four distinct weight loss regions (80−125, 150−308, 325−380, and 400−455 °C). These are due to the presence of moisture in the gel network (80−125 °C), degradation of cross-linker (150−308 °C), and dextrin moiety (325−380 °C).[12] The weight loss between 400 and 455 °C is probably owing to the breakdown of pNIPAm chains present in the xerogel.

The SEM analysis is extremely important to examine the surface topology and interior morphology of cross-linked xerogel and hydrogel.

The FE-SEM micrographs of dextrin and xerogel (c-Dxt/pNIPAm 8) are depicted in parts a and b, respectively, of Figure 3. It is obvious that dextrin (Figure 3a) demonstrated a fine oval shaped granular morphology. The insertion of MBA as cross-linker onto the hydrogelator matrix leads to rough and microporous morphology of c-Dxt/pNIPAm xerogel (Figure 3b). This microporous morphology of c-Dxt/pNIPAm hydrogel can play an important role for controlled swelling nature as well as for sustained drug release. The various interconnected pores and the cross-linked network are obvious in the E-SEM image of c-Dxt/pNIPAm 8 hydrogel (Figure 3c).

The physical properties of c-Dxt/pNIPAm xerogel, drugs, and the drugs' polymorphism after tablet formation were studied using XRD analyses. The c-Dxt/pNIPAm 8 xerogel showed (Figure S5a, Supporting Information) a broad characteristic peak at 2θ = 14.5°, indicating that the

DOI: 10.1021/acsami.5b02975
ACS Appl. Mater. Interfaces 2015, 7, 14338−14351

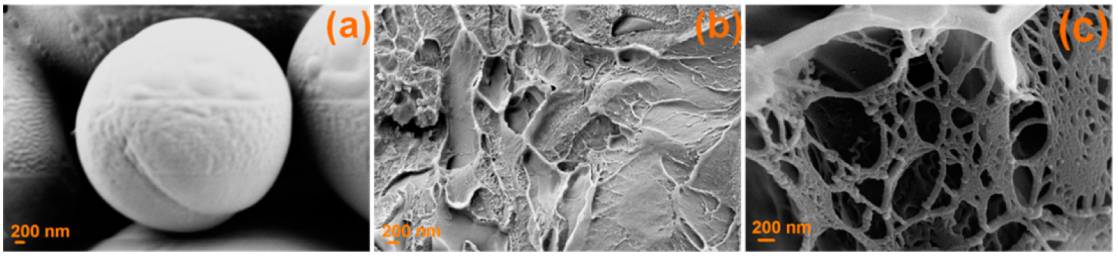

Figure 3. FE-SEM images of (a) dextrin and (b) c-Dxt/pNIPAm 8 xerogel. E-SEM image of (c) c-Dxt/pNIPAm 8 hydrogelator.

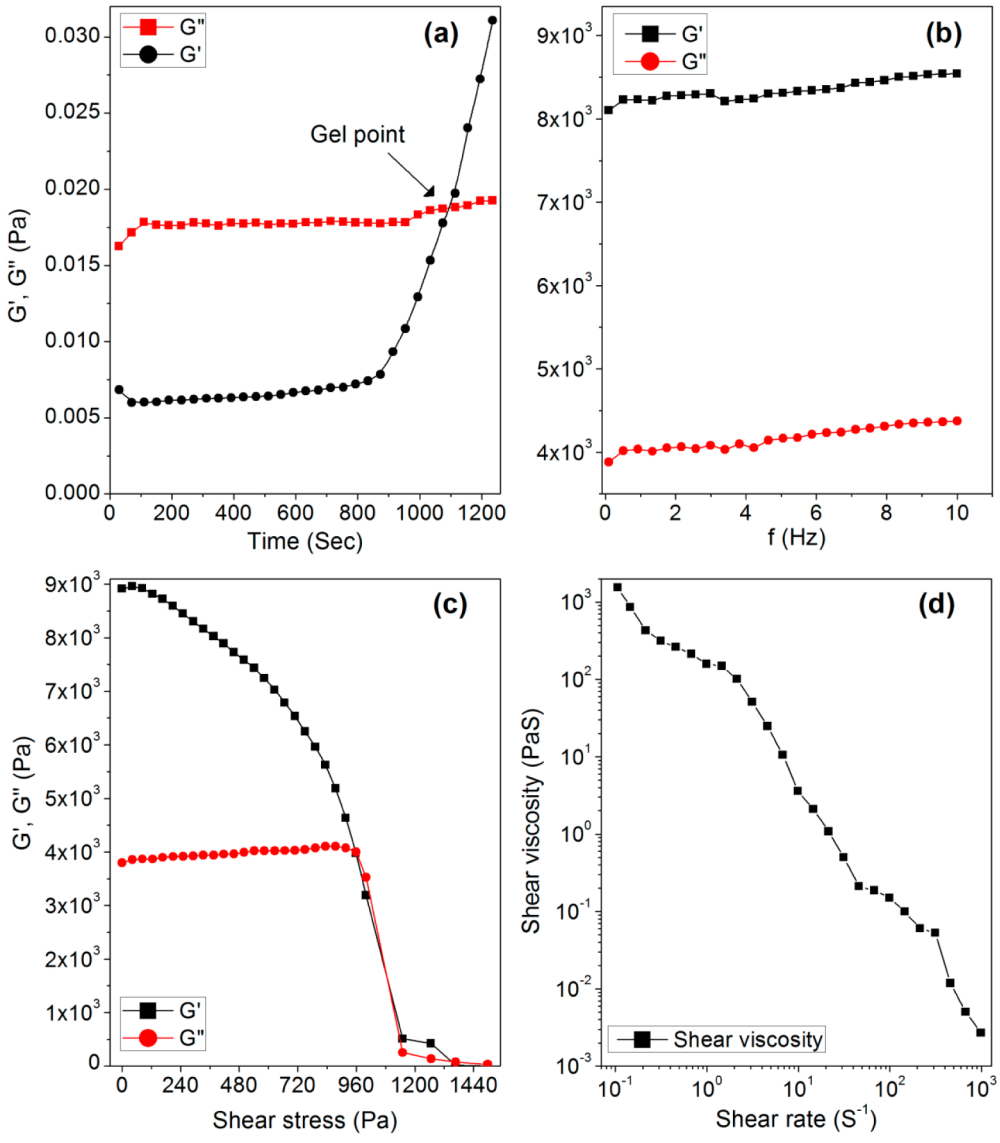

Figure 4. Rheological study of c-Dxt/pNIPAm 8 hydrogel: (a) G', G'' vs time, (b) G', G'' vs frequency, (c) G', G'' vs shear stress, and (d) shear viscosity vs shear rate.

hydrogelator is amorphous in nature. Ornidazole (Figure S5b, Supporting Information) showed peaks at 2θ = 13.5, 16.2, 21.1, 23.2, 24.4, 25.8, 27.6, 30.7, and 32.6°, and the corresponding peaks for ciprofloxacin (Figure S5d, Supporting Information) are 2θ = 19.23, 26.25, and 29.28° because of their crystalline behavior. The ornidazole tablet formulation suggests that the peak of cross-linked xerogel was merged with that of ornidazole (Figure S5c, Supporting Information). As a result, peak intensities of drugs diminished and few peaks disappeared, which indicates good compatibility between ornidazole and the matrix. Besides, for ciprofloxacin tablet, the xerogel peak shifted toward a higher value (from 14.5 to 20.7°) and all the peaks of ciprofloxacin were merged with the peak of c-Dxt/pNIPAm xerogel, which makes it difficult to evaluate the detection limit of the crystal (Figure S5e, Supporting Information). This behavior suggests good compatibility between ciprofloxacin and the c-Dxt/pNIPAm 8 hydrogel.

DOI: 10.1021/acsami.5b02975
ACS Appl. Mater. Interfaces 2015, 7, 14338−14351

UV−vis−NIR spectra reveal that the characteristics peaks of ornidazole and ciprofloxacin are attributed to the conjugation in the imidazole ring and quinolone ring, respectively (Figure S6, Supporting Information). The tablet formulations showed blue shifts (for ornidazole, Figure S6a in the Supporting Information, 371.6 nm→ 338.7 nm; for ciprofloxacin, Figure S6b in the Supporting Information, 366.9 nm → 361.8 nm), which corroborate that physical interactions predominate between drugs and the hydrogelator as proposed in Figure S2 in the Supporting Information.

3.3. Rheology Study. *Gel Kinetics.* Time sweep experiments were carried out to determine the kinetics of gel formation at 75 °C. As shown in Figure 4a, both the elastic (G') and viscous moduli (G'') increased over time. The point at which G' intersects G'' (i.e., ∼1095 s) is typically used as the gelling time (t_{gel}).

Rheological experiments were also performed to examine the effects of cross-linking on the c-Dxt/pNIPAm 8 hydrogelator mechanical properties. G' was plotted as a function of frequency, which was significantly higher than G'', indicating the gel state of the c-Dxt/pNIPAm 8 at the experimental conditions (Figure 4b). Further, the gel strength of the hydrogel was determined from the G' and G'' vs shear stress plot (Figure 4c). Both G' and G'' fall after a certain stress value signifying the gel−liquid transition. Both G' and G'' rapidly decreased, suggesting collapse of the network structure. This is mainly because of the fact that, with a rise in shear stress, the entanglements of the network hydrogel deformed.[44] These result in the fall in modulus values. The threshold stress above which the breakdown of the gel occurs is called the yield stress (σ). The σ for c-Dxt/pNIPAm 8 hydrogel is ∼1000 Pa. Additionally, the plot of shear viscosity vs shear rate (Figure 4d) indicates the non-Newtonian shear thinning behavior of c-Dxt/pNIPAm 8.

3.4. Biodegradation Study. Figure 5 represents the biodegradation study result for c-Dxt/pNIPAm 8 film after 0, 3, 7, 14, and 21 days. Hen egg white lysozyme possesses an analogous main chain formation and binding subsites as human lysozyme and PBS to stimulate in vivo conditions.[42] During the biodegradation study, it was observed that the mass of the cross-linked hydrogel gradually declined. Lysozymes degrade the polysaccharides through enzymatic hydrolysis of the glycosidic bonds.[42,43,45] Once the number of suitable sites was reduced; the rate of degradation was declined between 7 and 21 days. On the other hand, hydrogel film which remained in the PBS solution without lysozyme showed swelling behavior rather than dissolution and kept intact the weight the same as before (Figure 5).

3.5. In Vitro Cytotoxicity Study and Cell Proliferation. The synthesized c-Dxt/pNIPAm 8 hydrogelator is anticipated for oral drug delivery applications. Hence, it is essential to investigate the cytocompatibility of the material. To investigate cell proliferation, variation in DNA content was determined after specific time intervals (first, third, and seventh days).

The DNA amount was enhanced with a rise in incubation period for both synthesized hydrogel and the tissue culture plate (TCP). However, cells on c-Dxt/pNIPAm 8 hydrogel displayed higher proliferation efficiency (Figure 6a). This is due to the hydrophilic nature of c-Dxt/pNIPAm, which swells to form 3-D networks. This offers a broad surface for cells to grow up and proliferate, whereas cell proliferation is limited on the 2-D surface of the tissue culture plate. These higher numbers of cell population of c-Dxt/pNIPAm 8 signify higher cell viability

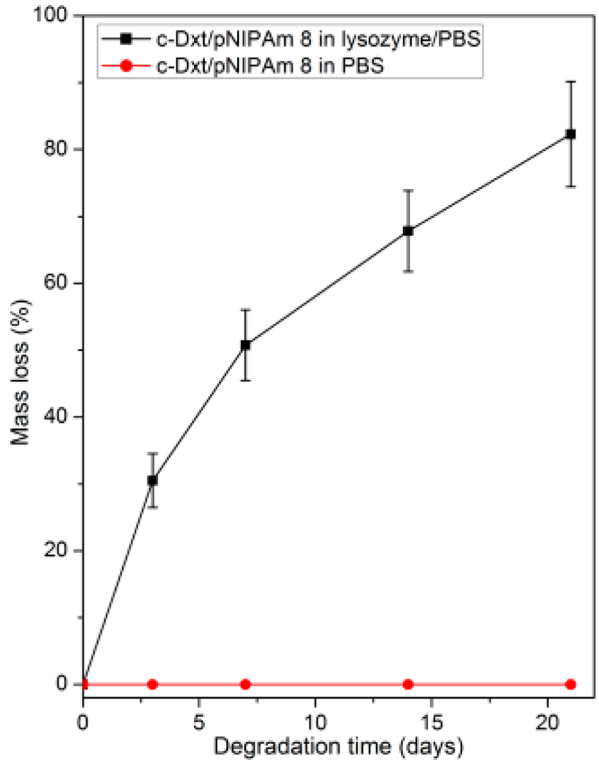

Figure 5. Progressive mass loss of c-Dxt/pNIPAm 8 xerogel films (■) in lysozyme/PBS and (●) in PBS only. Results represented are mean ± SD, n = 3.

of the cross-linked hydrogelator than the TCP and confirm the nontoxicity of c-Dxt/pNIPAm. Fluorescent images of mesenchymal stem cells on lysine coated coverslip and polymer pellet after 3 and 7 days are shown in Figure 6b. Cells of both groups adhered well on their respective substrates on the third day. After 7 days, the cells displayed well-spread morphology with a prominent nucleus, further confirming the cytocompatibility of the material.

3.6. Swelling Characteristics of Hydrogel. From Figure S7 in the Supporting Information, it has been observed that with progress in time, the % ESR of dextrin declined, suggesting its solubility in aqueous media. In contrast, c-Dxt/pNIPAm hydrogel achieved its equilibrium swelling at ∼6 h (Supporting Information, Figure S7) and % ESR values of hydrogels are higher than that of dextrin. This is because of the incorporation of pNIPAm and cross-linker in the gel network, which improved the hydrophilicity of the network and increased the surface area for water diffusion (due to 3-D network). Besides, the porous surface of c-Dxt/pNIPAm also assists the diffusion of water into the network.[23] Among the various synthesized hydrogelators, c-Dxt/pNIPAm 8 demonstrates the lowest % ESR (Table 1 and Supporting Information, Figure S7) because of its higher % CR (Table 1). This makes the hydrogel structure more stiff and opaque, resulting in less swelling than that of hydrogelators with lower % CR.

pH-Responsive Behavior. The pH-sensitive swelling characteristics of c-Dxt/pNIPAm hydrogelators were investigated, and results are represented in Figure S7a−c in the Supporting Information. The % ESR in alkaline medium was found to be higher than that of acidic medium (Table 1). This is mainly because of the protonation of hydrophilic groups present in c-Dxt/pNIPAm in acidic media (i.e., pH 1.2), which deterred the

DOI: 10.1021/acsami.5b02975
ACS Appl. Mater. Interfaces 2015, 7, 14338−14351

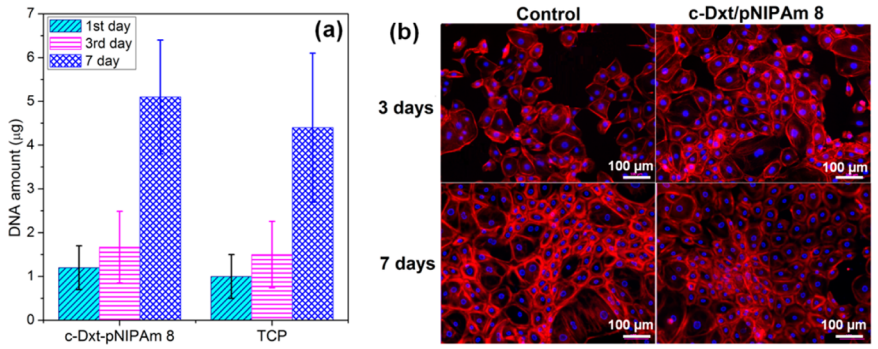

Figure 6. (a) Cell proliferation result of c-Dxt/pNIPAm 8 hydrogelator by DNA quantification assay (results represented are mean ± SD, $n = 3$) and (b) cellular attachment on pellet of c-Dxt/pNIPAm 8 hydrogel and control (lysine coated slides) by rhodamine phalloidin and DAPI assay at different time periods.

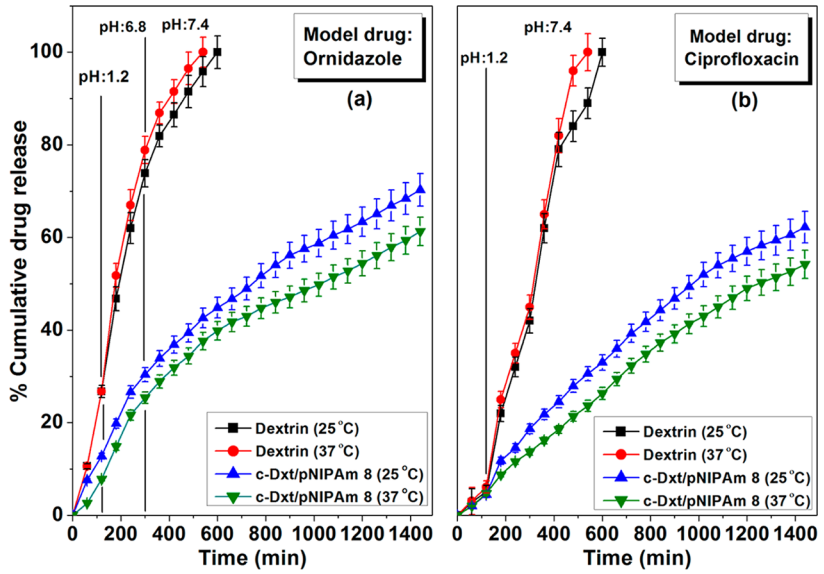

Figure 7. In vitro release of (a) ornidazole from dextrin and c-Dxt/pNIPAm 8 and (b) ciprofloxacin from dextrin and c-Dxt/pNIPAm 8. Results represented are mean ± SD, $n = 3$.

formation of H-bonding with water.[12] This will result in lower % ESR. In alkaline media (i.e., pH 7.4), all the hydrophilic groups remain free to form more H-bonding with water, resulting in higher % ESR.[12]

Thermoresponsive Behavior. The temperature-sensitive swelling nature of the cross-linked hydrogelators was also studied (Supporting Information, Figure S7c,d). It has been observed that, with an increase in temperature, % ESR decreased. NIPAm contains two parts: one is hydrophilic, i.e., −NHCO−, and the other is hydrophobic, i.e., $-CH(CH_3)_2$. At 25 °C (below the LCST), the hydrophilic groups of c-Dxt/pNIPAm hydrogelator form intermolecular hydrogen bonding with water molecules, which makes the penetrated water into the hydrogelator matrix at the bound state.[1] At 37 °C (above LCST), water molecules will acquire enthalpy and some of the hydrophilic groups in the hydrogelator turn into intramolecular hydrogen bonding, resulting in the increase in hydrophobic force among the polymer chains. This results in higher % ESR at lower temperature compared to higher temperature.

Swelling Kinetics. The rate of water absorption by c-Dxt/pNIPAm hydrogelators at various pHs and temperatures was determined using the Voigt model. At 37 °C and pH 7.4, the rate parameter value τ (Table S2, Supporting Information) is lower than those for pH 1.2 and pH 6.8, which indicates that the rate of diffusion of water molecules is higher in alkaline media compared to acidic media. Among the various hydrogels, c-Dxt/pNIPAm 8 has the highest τ value due to its highest % CR, which indicates the lowest rate of swelling. It was also observed that, at 25 °C, the rate parameter values (τ) (Table S2, Supporting Information) are lower than those at 37 °C, which signifies that the swelling rate at 25 °C is higher than at 37 °C.

3.7. In Vitro Ornidazole and Ciprofloxacin Release Study. *pH Responsive Drug Release Study.* Figure 7 demonstrates the percent cumulative drug (ornidazole and ciprofloxacin) release from c-Dxt/pNIPAm 8 and dextrin in various pH (1.2, 6.8, and 7.4) media at 25 and 37 °C. It is well-known that the release rate of a drug depends primarily on the chemical structure of the hydrogel as well as on the % ESR of hydrogels.[57] Higher % ESR values of hydrogels offer more surface for diffusion of drugs to the release media.[12] The water-soluble drugs are released from hydrogel based tablet formulations mainly through the dissolution process; a small quantity of drug is also released by erosion of the matrix.[12]

From Figure 7, it is apparent that the rate of ornidazole release is higher in alkaline media than that of acidic pH. This is because drugs remain at the collapsed state in the c-Dxt/pNIPAm 8 at pH 1.2 and thus swell less. Therefore, the drugs

DOI: 10.1021/acsami.5b02975
ACS Appl. Mater. Interfaces 2015, 7, 14338−14351

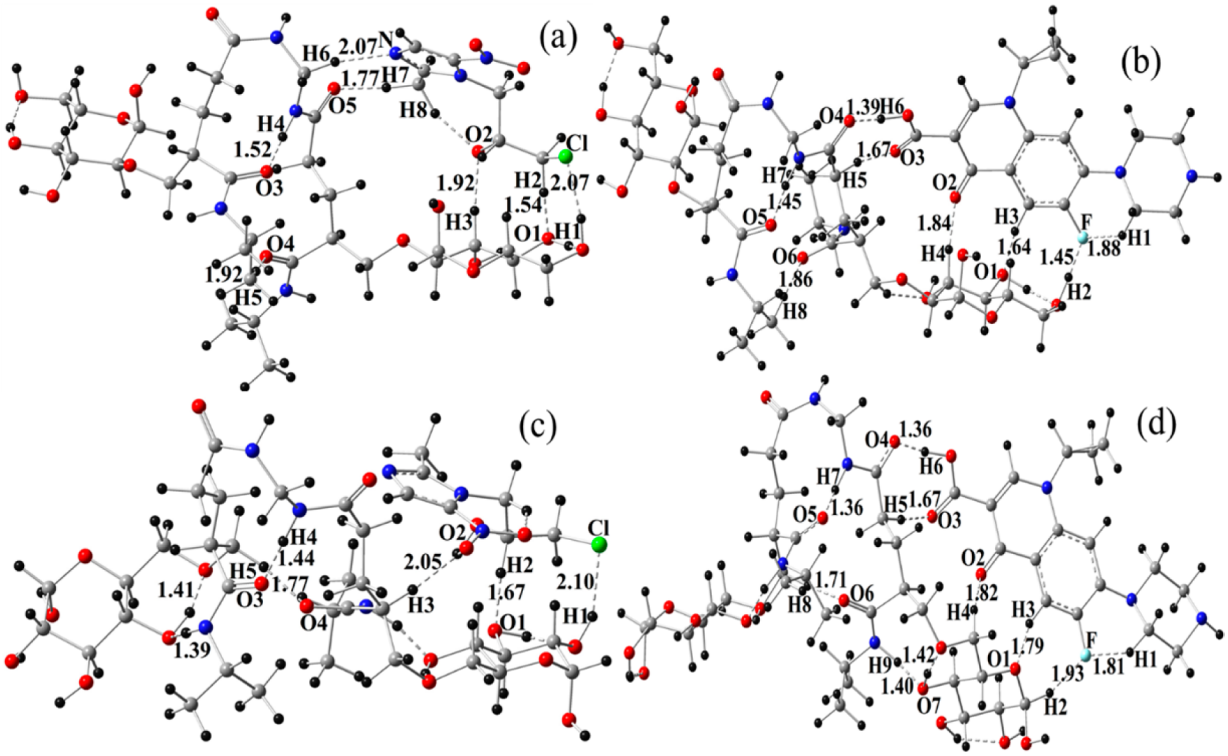

Figure 8. Optimized structures of (a) polymer 1@ornidazole, (b) polymer 1@ciprofloxacin, (c) polymer 2@ornidazole, and (d) polymer 2@ciprofloxacin calculated at DFT/B3LYP/STO-3G* level of theory.

will not be able to diffuse from the hydrogel into the media. Similarly, the ciprofloxacin release rate was also very much less at pH 1.2 compared to pH 7.4. However, at neutral/alkaline media, the hydrogels swelled rapidly. This results in an increase in drug diffusion from the matrix.[12] Consequently, at higher pH the rates of ornidazole and ciprofloxacin release were higher compared to acidic pH. Out of various hydrogelators, c-Dxt/pNIPAm 8 released the drugs (~70.30 ± 3.51% ornidazole and ~68.20 ± 3.41% ciprofloxacin release after 24 h) in a more controlled way than that of dextrin. Besides, due to the covalent attachment of cross-linker in the gel network, the percent erosion (Table S3, Supporting Information) of the hydrogel is much lower compared to dextrin, which also affects the sustained release behavior of ornidazole and ciprofloxacin.

Temperature Responsive Drug Release Study. From Figure 7, it was observed that, with a rise in temperature from 25 to 37 °C, the release of drugs (ornidazole and ciprofloxacin) from c-Dxt/pNIPAm 8 declined. As stated in section 3.6, at 25 °C % ESR was higher than that at 37 °C. Below LCST (25 °C) of pNIPAm, water molecules remain in the hydrogel matrix by intermolecular H-bonding as a bound state. Thus, the tendency to diffuse the water molecules into the hydrogel matrix would be greater compared to above LCST (37 °C). The enthalpy factor and the hydrophobic force make some water molecules free from the bound state. Similarly, as water penetration in c-Dxt/pNIPAm hydrogel is easier at 25 °C than at 37 °C, so the diffusion rate of ornidazole/ciprofloxacin from c-Dxt/pNIPAm to media as well as the percent cumulative drug release was greater at 25 °C than at 37 °C. This phenomenon has also been confirmed from diffusion coefficient values at different temperatures (Table S4, Supporting Information).

Thus, from ornidazole/ciprofloxacin release profiles from c-Dxt/pNIPAm hydrogel, it is apparent that grafting of pNIPAm on dextrin backbone followed by chemical cross-linking of MBA increased the hydrophilicity of the hydrogel that controlled the swelling nature, minimized the erosion rate, and subsequently released the drugs in a more controlled way.

Drug Release Kinetics. The release kinetics of ornidazole and ciprofloxacin from dextrin and c-Dxt/pNIPAm 8 hydrogel was investigated using zero order and first order kinetic models. (For details see Supporting Information.) The regression coefficient (R^2) values (Table S5, Supporting Information) obtained from the first order kinetic model are greater than those from the zero order kinetic model. This confirmed that the ornidazole release (pH 6.8 and pH 7.4) and ciprofloxacin release (pH 7.4) from dextrin and c-Dxt/pNIPAm hydrogel follow first order kinetics.

Mechanism of Drug Release. Drug release may happen from the hydrogel system through Fickian/non-Fickian/and case II diffusion.[58,59] The release phenomenon also depends on the mechanical strength of the hydrogel and external stimulus (such as pH, temperature, ionic strength) along with the chemical properties of the hydrogel matrix. We have used different mathematical models, including the Korsmeyer–Peppas model,[60] the Higuchi model,[61] the Hixson–Crowell model,[62] and the nonlinear Kopcha model,[63] to predict the mechanism of ornidazole/ciprofloxacin release from dextrin and c-Dxt/pNIPAm hydrogelator. (Details of various models have been explained in Supporting Information.)

For the ornidazole release from c-Dxt/pNIPAm hydrogel in both media (pH 6.8 and 7.4) and the ciprofloxacin release (pH 7.4), the diffusion exponent (n) values (Table S5, Supporting Information) obtained from the Korsmeyer–Peppas model are between 0.45 and 0.89, which implies that non-Fickian diffusion mechanism; i.e., the combination of diffusion and erosion of the matrix predominate. Besides, the R^2 values (Table S5, Supporting Information) of the Higuchi and Hixson–Crowell models suggest that the drug release follows the Higuchi model

DOI: 10.1021/acsami.5b02975
ACS Appl. Mater. Interfaces 2015, 7, 14338–14351

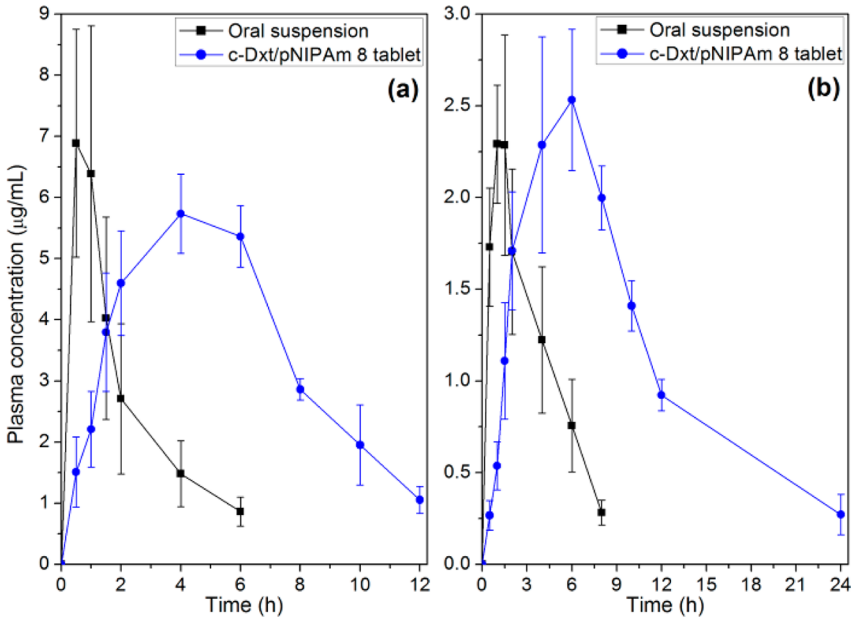

Figure 9. In vivo release of (a) ciprofloxacin and (b) ornidazole from dextrin and c-Dxt/pNIPAm 8 tablets. Results represented are mean ± SD, n = 3.

rather than the Hixson−Crowell model; i.e., the diffusion process is mainly responsible for ornidazole and ciprofloxacin release from c-Dxt/pNIPAm hydrogel.

Furthermore, the nonlinear Kopcha model (A and B values) evaluates the quantitative contributions of the diffusion and erosion processes for drug release. In the case of ornidazole release, the exponent values (Table S5, Supporting Information) signify that, at pH 6.8, a major percentage of the drug was released through the diffusion process while percent erosion has a minute contribution. At pH 7.4, the exponent values (Table S5, Supporting Information) confirmed that the erosion process equally contributes along with the diffusion process for ornidazole release. On the other hand, the values of the diffusion exponent (A) and the erosion exponent (B) (Table S5, Supporting Information) obtained from the Kopcha model for the ciprofloxacin release at pH 7.4 indicate that both diffusion and erosion processes are responsible for the release pattern.

Thus, from above explanations, it is apparent that non-Fickian diffusion is the main mechanism for release of both ornidazole and ciprofloxacin from c-Dxt/pNIPAm hydrogelator.

3.8. Stability Study. To investigate how the quality of ornidazole/ciprofloxacin in tablet formulation fluctuates with time under the influence of various factors such as temperature/humidity, a stability study of the prepared ornidazole/ciprofloxacin tablets was executed.[12,44] It is obvious from the drug stability results [FTIR spectra (Figure S8, Supporting Information), XRD analyses (Figure S9, Supporting Information), and release characteristics (initially and after 3 months, Figure S10 and Tables S6 and S7, Supporting Information)] that ∼97% ornidazole and ∼98% ciprofloxacin remain stable for up to 3 months in c-Dxt/pNIPAm 8 hydrogel.

3.9. Computational Study. *Optimization.* Polymer 1 (pNIPAm cross-linked dextrin via secondary alcoholic group), polymer 2 (pNIPAm cross-linked dextrin via primary alcoholic group), ciprofloxacin, and ornidazole were fully optimized in the gaseous state employing the DFT/B3LYP/STO-3G* level of theory in its unrestricted form and shown in Figure S11 in the Supporting Information. Both polymeric structures (polymer 1 and polymer 2) were dominated by intramolecular H-bonding. Intramolecular H-bonding allows both types of polymeric chains to adopt similar kinds of spatial arrangement, while dextrin molecules are trans to each other. Grafting of pNIPAm in the dextrin backbone via the primary alcoholic group facilitates forming more intramolecular H-bonding in the polymer 2 structure, which makes the structure more compact in comparison to the polymer 1 structure.

Binding Geometries of c-Dxt/pNIPAm Hydrogel−Drug Complexes and Interaction Energies. The optimized electronic structures of c-Dxt/pNIPAm hydrogelator and drug complexes under investigation are displayed in Figure 8. All the displayed hydrogel−drug complexes showed a number of intra- and intermolecular H-bond interactions of O−H···X, O−H···O, and N−H···O types (where X = Cl and F). Various types of H-bonding indicate the properties of hydrogel−drug interaction to a large extent. Inter- and intramolecular H-bonding distances present in c-Dxt/pNIPAm hydrogel@drug complexes are shown in Tables S8 and S9 in the Supporting Information. Due to the large number of intramolecular H-bonds in polymer 2, it is more compact and energetically more stable in comparison to polymer 1. From Table S10 in the Supporting Information it is obvious that the energetically polymer 2 structure is (−36.0557 kcal/mol) more stable than the polymer 1 structure.

By investigating the nature of H-bonding exist between the polymers with ornidazole and ciprofloxacin, it is apparent that ciprofloxacin always shows a stronger interaction than ornidazole. This is because of the stronger H-bonding nature of O−H···F than O−H···Cl. Between polymer 1 and polymer 2, polymer 1 demonstrates much more affinity towards the drugs ornidazole and ciprofloxacin than polymer 2. This can be explained by the fact that, in polymer 1, grafting of poly(*N*-isopropylacrylamide) (pNIPAm) proceeded on the dextrin backbone via a secondary alcoholic group, which makes the

DOI: 10.1021/acsami.5b02975
ACS Appl. Mater. Interfaces 2015, 7, 14338−14351

drug-receiving pocket more appropriate in size for small drugs like ornidazole and ciprofloxacin.

In polymer 2 the larger drug-receiving pocket makes the polymer2@ornidazole complex (ΔE = −9.74625 kcal/mol, zero point corrected energy $\Delta E_{corrected}$ = −7.36445 kcal/mol) less effective for H-bonding than the polymer1@ornidazole complex (ΔE = −21.45633 kcal/mol, zero point corrected energy $\Delta E_{corrected}$ = −18.70417 kcal/mol). The above observation was also supported by the number and reduced intermolecular H-bond distance in the polymer1@ornidazole complex (Tables S8 and S9, Supporting Information) than in the polymer2@ornidazole complex.

The comparatively larger drug molecule ciprofloxacin fits in a similar way with polymer 1 and polymer 2, which is reflected from their close complexation energies (Table S11, Supporting Information). For polymer1@ ciprofloxacin, the complexation energy ΔE = −39.0360294 kcal/mol and the zero point corrected energy $\Delta E_{corrected}$ = −34.697510 kcal/mol, while for polymer2@ciprofloxacin, the complexation energy ΔE = −30.5132 kcal/mol and the zero point corrected energy $\Delta E_{corrected}$ = −28.446 kcal/mol.

Gas phase calculation concludes that ciprofloxacin showed much higher affinity towards the c-Dxt/pNIPAm hydrogel unit than ornidazole. If grafting of pNIPAm on the dextrin backbone proceeds through a secondary alcoholic group, then it will display a stronger binding with small drugs like ornidazole. This complexation energy also showed a shifting in the vibrational frequencies in the complexes, which was noticed by examining the IR frequencies of the unbound and bound complexes.

3.10. In Vivo Pharmacokinetic Study of Ciprofloxacin and Ornidazole. Oral suspensions and the tablet dosage form of ciprofloxacin equivalent to 30 mg/kg body weight were given to group I and group II, respectively. Oral suspension and the tablet dosage form of ornidazole equivalent to 30 mg/kg body weight were administered to group III and group IV, respectively. The plasma drug concentrations for ciprofloxacin and ornidazole were periodically measured for 12 and 24 h as shown in parts a and b, respectively, of Figure 9.

The pharmacokinetic parameters were determined using noncompartmental analysis. The C_{max}, T_{max}, AUC_{0-t}, $AUC_{0-\infty}$, K_{el}, $T_{1/2}$, AUMC, and MRT values of all formulations of ciprofloxacin and ornidazole are represented in Table S12 in the Supporting Information. The time required to achieve the peak plasma concentration (T_{max}) of oral suspension was greater compared to that for the sustained release tablet dosage form in both drugs. This indicates the sustained release nature of the tablet dosage form. This property was obvious, because of the formation of cross-linked hydrogel matrix. The peak plasma concentration (C_{max}) of ciprofloxacin was significantly low for tablet dosage form as compared to oral suspension, indicating the lower rate of absorption which was a main goal to be achieved in the case of sustained release dosage form (Table S12, Supporting Information).

No significant difference was observed between the oral suspension and the sustained release tablet dosage form of ornidazole in the case of C_{max} (Table S12, Supporting Information). The extent of absorption should be greater compared to that for the oral suspension, which is another main goal to be achieved in the case of ideal sustained release dosage form. Determination of area under the curve (AUC) is the quantification of the extent of absorption. In our study, AUC values for tablet dosage forms of both drugs were very large as compared to those for the oral suspensions. This suggests that the cross-linked hydrogel matrix was efficiently able to control the drug release in vivo. The high standard deviation and percentage coefficient variation in both cases may be minimized by increasing the number of animals per group, but it is a regulatory constraint in our country.

4. CONCLUSIONS

A novel chemically cross-linked hydrogelator (c-Dxt/pNIPAm) was successfully developed using dextrin, MBA, and *N*-isopropylacrylamide through free radical polymerization followed by Michael type addition reaction. Various characterization techniques such as FTIR spectroscopy, ^{1}H and ^{13}C NMR spectral analysis, TGA analysis, and FE-SEM/E-SEM analyses confirm the development of cross-linked hydrogelator. The stimulus responsiveness of the hydrogel was verified by determining the % ESR at various temperatures and in different buffer media. Cell viability study and degradation study imply that c-Dxt/pNIPAm hydrogel is nontoxic for mesenchymal stem cells (hMSCs) and degradable in nature. Interestingly, the drug release profiles suggest that c-Dxt/pNIPAm released ornidazole and ciprofloxacin in a controlled way. FTIR spectra, XRD analysis, UV−vis−NIR spectra, and computational study indicate that there is excellent compatibility between the drugs and the hydrogel matrix. Besides, the stability study implies that ∼97% ornidazole and ∼98% ciprofloxacin remain stable in the tablet formulations for up to 3 months. Finally, the pH and temperature responsiveness, noncytoxicity, biodegradability, and good compatibility between the drugs and the matrix along with the controlled release behavior would make the hydrogel an excellent alternative for controlled release of ornidazole and ciprofloxacin.

■ ASSOCIATED CONTENT

Supporting Information

Details of biodegradation study, in vitro cytotoxicity study, swelling and deswelling study; details of tablet preparation method; various drug release kinetics and mechanism models; percent erosion; details of stability study method; pharmacokinetic analysis of in vivo release study, FTIR spectra (Figure S1), drug−matrix interaction (Figure S2); ^{1}H NMR spectrum of NIPAm (Figure S3), cross-linking density of c-Dxt/pNIPAm 8 hydrogelator (Table S1); TGA analysis (Figure S4); XRD analysis (Figure S5); UV−vis−NIR study (Figure S6); swelling characteristics of dextrin and various hydrogelators in different pHs and temperatures (Figure S7); swelling kinetics parameters (Table S2); percent erosion (Table S3); diffusion coefficient values (Table S4); release parameters (Table S5); stability study results (Figures S8−S10, Tables S6 and S7); optimized electronic structure (Figure S11); H-bonding distance data (Tables S8 and S9); physical parameters of various complexes (Table S10); complexation energy (Table S11); in vivo drug release data (Table S12). The Supporting Information is available free of charge on the ACS Publications website at DOI: 10.1021/acsami.5b02975.

■ AUTHOR INFORMATION

Corresponding Author

*Tel.: +91-326-2235769. Fax: 0091-326-2296615. E-mail: sagarpal1@hotmail.com or pal.s.ac@ismdhanbad.ac.in.

Notes

The authors declare no competing financial interest.

DOI: 10.1021/acsami.5b02975
ACS Appl. Mater. Interfaces 2015, 7, 14338−14351

■ ACKNOWLEDGMENTS

D.D. wishes to acknowledge the University Grant Commission, New Delhi, India (Reference No.19-06/2011(i) EU-IV; Sr. No. 2061110303, dated Nov 30, 2011) for providing financial assistance under the Junior Research Fellowship Scheme. The corresponding author (S.P.) acknowledged the financial support from SERB, Department of Science & Technology, New Delhi, India in form of a research grant (File No. - EMR/2014/000471).

■ REFERENCES

(1) Gau, B. L.; Gau, Q. Y. Preparation and Properties of a pH/Temperature-Responsive Carboxymethyl Chitosan/Poly(N-isopropylacrylamide) Semi-IPN Hydrogel for Oral Delivery of Drugs. *Carbohydr. Res.* **2007**, *342*, 2416−2422.

(2) Shalaby, W. S. W.; Blevins, W. E. Polymeric Drugs and Drug Delivery Systems. *ACS Symp. Ser.* **1991**, *469*, 237−248.

(3) Lan, W.; Chunhua, C.; Jiaping, L.; Tao, C. Dual-Drug Delivery System based on Hydrogel/Micelle Composites. *Biomaterials* **2009**, *30*, 2606−2613.

(4) Mok, H.; Park, J. W.; Park, T. G. Enhanced Intracellular Delivery of Quantum Dot and Adenovirus Nanoparticles Triggered by Acidic pH via Surface Charge Reversal. *Bioconjugate Chem.* **2008**, *19*, 797−801.

(5) He, C.; Kim, S. W.; Lee, D. S. In Situ Gelling Stimuli-Sensitive Block Copolymer Hydrogels for Drug Delivery. *J. Controlled Release* **2008**, *127*, 189−207.

(6) Nguyen, D. N.; Raghavan, S. S.; Tashima, L. M.; Lin, E. C.; Fredette, S. J.; Langer, R. S. Enhancement of Poly (Ortho Ester) Microspheres for DNA Vaccine Delivery by Blending with Poly (Ethylenimine). *Biomaterials* **2008**, *29*, 2783−2793.

(7) Bae, V.; Kataoka, K. Preparation, Characterization and Anticoagulation of Curcumin-Eluting Controlled Biodegradable Coating Stents. *J. Controlled Release* **2006**, *116*, 49−50.

(8) Kono, H.; Teshirogi, T. Cyclodextrin-Grafted Chitosan Hydrogels for Controlled Drug Delivery. *Int. J. Biol. Macromol.* **2015**, *72*, 299−308.

(9) Lai, W. F.; Shum, H. C. Hypromellose-Graft-Chitosan and Its Polyelectrolyte Complex as Novel Systems for Sustained Drug Delivery. *ACS Appl. Mater. Interfaces* **2015**, *7*, 10501−10510.

(10) Watanabe, M.; Kawano, K.; Toma, K.; Hattori, Y.; Maitani, V. In Vivo Antitumor Activity of Camptothecin Incorporated in Liposomes Formulated with an Artificial Lipid and Human Serum Albumin. *J. Controlled Release* **2008**, *127*, 231−238.

(11) Tamilvanan, S.; Venkateshan, N.; Ludwig, A. The Potential of Lipid- and Polymer-based Drug Delivery Carriers for Eradicating Biofilm Consortia on Device-Related Nosocomial Infections. *J. Controlled Release* **2008**, *128*, 2−24.

(12) Das, D.; Das, R.; Ghosh, P.; Panda, A. B.; Pal, S. Dextrin Crosslinked with Poly(HEMA): A Novel Hydrogel for Colon Specific Delivery of Ornidazole. *RSC Adv.* **2013**, *3*, 25340−25350.

(13) Das, D.; Pal, S. Modified Biopolymer-Dextrin Based Crosslinked Hydrogels: Application in Controlled Drug Delivery. *RSC Adv.* **2015**, *5*, 25014−25050.

(14) Huynh, D. P.; Im, G. J.; Chae, S. Y.; Lee, K. C.; Lee, D. S. Controlled Release of Insulin from pH/Temperature-Sensitive Injectable Pentablock Copolymer Hydrogel. *J. Controlled Release* **2009**, *137*, 20−24.

(15) Im, J. S.; Bai, B. C.; In, S. J.; Lee, Y. S. Improved Photodegradation Properties and Kinetic Models of a Solar-Light-Responsive Photocatalyst when Incorporated into Electrospun Hydrogel Fibers. *J. Colloid Interface Sci.* **2010**, *346*, 216−221.

(16) Jin, S.; Gu, J.; Shi, Y.; Shao, K.; Yu, X.; Yue, G. Preparation and Electrical Sensitive Behavior of Poly (N-vinylpyrrolidone-co-Acrylic acid) Hydrogel with Flexible Chain Nature. *Eur. Polym. J.* **2013**, *49*, 1871−1880.

(17) Matsusaki, M.; Akashi, M. Novel Functional Biodegradable Polymer IV: pH-Sensitive Controlled Release of Fibroblast Growth Factor-2 from a Poly (γ-glutamic acid)-Sulfonate Matrix for Tissue Engineering. *Biomacromolecules* **2005**, *6*, 3351−3356.

(18) Das, D.; Pal, S. Dextrin/Poly (HEMA): pH Responsive Porous Hydrogel for Controlled Release of Ciprofloxacin. *Int. J. Biol. Macromol.* **2015**, *72*, 171−178.

(19) Ju, H. K.; Kim, S. Y.; Lee, Y. M. pH/Temperature-Responsive Behaviours of Semi-IPN and Comb-Type Graft Hydrogels Composed of Alginate and Poly (N-Isopropylacrylamide). *Polymer* **2001**, *42*, 6851−6857.

(20) Qiu, B.; Stefanos, S.; Ma, J.; Lalloo, A.; Perry, A. B.; Leibowitz, M. J.; Sinko, P. J.; Stein, S. A Hydrogel Prepared by In Situ Crosslinking of a Thiol-Containing Poly(Ethylene Glycol)-Based Copolymer: A New Biomaterial for Protein Drug Delivery. *Biomaterials* **2003**, *24*, 11−18.

(21) Corkhill, P. H.; Hamilton, C. J.; Tighe, B. J. Synthetic Hydrogels VI. Hydrogel Composites as Wound Dressings and Implant Materials. *Biomaterials* **1989**, *10*, 3−10.

(22) Wilson, A. N.; Elie, A. G. Targeting Homeostasis in Drug Delivery Using Bioresponsive Hydrogel Microforms. *Int. J. Pharm.* **2014**, *461*, 214−222.

(23) Das, D.; Das, R.; Mandal, J.; Ghosh, A.; Pal, S. Dextrin Crosslinked with Poly (Lactic acid): A Novel Hydrogel for Controlled Drug Release Applications. *J. Appl. Polym. Sci.* **2014**, *131*, 40039.

(24) Hoffman, A. S. Hydrogels for Biomedical Applications. *Adv. Drug Delivery Rev.* **2012**, *64*, 18−23.

(25) Nicodemus, G. D.; Bryant, S. J. Cell Encapsulation in Biodegradable Hydrogels for Tissue Engineering Applications. *Tissue Eng., Part B* **2008**, *14*, 149−165.

(26) Tanase, C. P.; Albulescu, R.; Neagu, M. Application of 3D Hydrogel Microarrays in Molecular Diagnostics: Advantages and Limitations. *Expert Rev. Mol. Diagn.* **2011**, *11*, 461−464.

(27) Brandl, F.; Kastner, F.; Gschwind, R. M.; Blunk, T.; Teßmar, J.; Göpferich, A. Hydrogel-Based Drug Delivery Systems: Comparison of Drug Diffusivity and Release Kinetics. *J. Controlled Release* **2010**, *142*, 221−228.

(28) Hoare, T. R.; Kohane, D. S. Hydrogels in Drug Delivery: Progress and Challenges. *Polymer* **2008**, *49*, 1993−2007.

(29) Shen, M.; Li, L.; Sun, Y.; Xu, J.; Guo, X.; Prud'homme, R. K. Rheology and Adhesion of Poly(acrylic acid)/Laponite Nanocomposite Hydrogels as Biocompatible Adhesives. *Langmuir* **2014**, *30*, 1636−1642.

(30) Haraguchi, K.; Farnworth, R.; Ohbayashi, A.; Takehisa, T. Compositional Effects on Mechanical Properties of Nanocomposite Hydrogels Composed of Poly (N,N-Dimethylacrylamide) and Clay. *Macromolecules* **2003**, *36*, 5732−5741.

(31) Haraguchi, K.; Li, H. J.; Song, L.; Murata, K. Tunable Optical and Swelling/Deswelling Properties Associated with Control of the Coil-to-Globule Transition of Poly (N-isopropylacrylamide) in Polymer−Clay Nanocomposite Gels. *Macromolecules* **2007**, *40*, 6973−6980.

(32) Li, L.; Gu, J.; Zhang, J.; Xie, Z.; Lu, Y.; Shen, L.; Dong, Q.; Wang, Y. Injectable and Biodegradable pH-Responsive Hydrogels for Localized and Sustained Treatment of Human Fibrosarcome. *ACS Appl. Mater. Interfaces* **2015**, *7*, 8033−8040.

(33) Molinos, M.; Carvalho, V.; Silva, D. M.; Gama, F. M. Development of a Hybrid Dextrin Hydrogel Encapsulating Dextrin Nanogel As Protein Delivery System. *Biomacromolecules* **2012**, *13*, 517−527.

(34) Frampton, J. E.; Plosker, G. L. Icodextrin: A Review of Its Use in Peritoneal Dialysis. *Drugs* **2003**, *63*, 2079−2105.

(35) Hirst, D. H.; Chicco, D.; German, L.; Duncan, R. Dextrins as Potential Carriers for Drug Targeting: Tailored Rates of Dextrin Degradation by Introduction of Pendant Groups. *Int. J. Pharm.* **2001**, *230*, 57−66.

(36) Chen, G. H.; Hoffman, A. S. Graft Copolymers That Exhibit Temperature-Induced Phase Transitions Over a Wide Range of pH. *Nature* **1995**, *373*, 49−52.

DOI: 10.1021/acsami.5b02975
ACS Appl. Mater. Interfaces 2015, 7, 14338−14351

(37) Yamashita, K. J.; Nishimura, T.; Nango, M. Preparation of IPN-Type Stimuli-Responsive Heavy-Metal-Ion Adsorbent Gel. *Polym. Adv. Technol.* **2003**, *14*, 189−194.
(38) Chen, M. Q.; Serizaw, T.; Akashi, M. Polystyrene Microspheres with Poly (N-Isopropylacrylamide) Branches on Their Surfaces: Size Control Factors and Thermosensitive Behavior. *Polym. Adv. Technol.* **1999**, *10*, 120−126.
(39) Shi, X. Y.; Li, J. B.; Sun, C. M.; Wu, S. K. Water-Solution Properties of a Hydrophobically Modified Poly(N-Isopropylacrylamide). *J. Appl. Polym. Sci.* **2000**, *75*, 247−255.
(40) Chen, C. W.; Akashi, M. Synthesis, Characterization, and Catalytic Properties of Colloidal Platinum Nanoparticles Protected by Poly (N-Isopropylacrylamide). *Langmuir* **1997**, *13*, 6465−6472.
(41) Huh, K. M.; Hashi, J.; Ooya, T.; Yui, N. Synthesis and Characterization of Dextran Grafted with Poly (N-Isopropylacrylamide-co-N,N-Dimethyl-Acrylamide). *Macromol. Chem. Phys.* **2000**, *201*, 613−619.
(42) Freier, T.; Koh, H. S.; Kazazian, K.; Shoichet, M. S. Controlling Cell Adhesion and Degradation of Chitosan Films by N-Acetylation. *Biomaterials* **2005**, *26*, 5872−5878.
(43) Justin, R.; Chen, B. Characterization and Drug Release Performance of Biodegradable Chitosan-Graphene Oxide Nanocomposites. *Carbohydr. Polym.* **2014**, *103*, 70−80.
(44) Das, D.; Ghosh, P.; Dhara, S.; Panda, A. B.; Pal, S. Dextrin and Poly (Acrylic Acid) Based Biodegradable, Non-Cytotoxic, Chemically Crosslinked Hydrogel for Sustained Release of Ornidazole and Ciprofloxacin. *ACS Appl. Mater. Interfaces* **2015**, *7*, 4791−4803.
(45) Das, R.; Das, D.; Ghosh, P.; Dhara, S.; Panda, A. B. Development and Application of a Nanocomposite Derived from Crosslinked HPMC and Au Nanoparticles for Colon Targeted Drug Delivery. *RSC Adv.* **2015**, *5*, 27481−27490.
(46) Ghosh, P.; Rameshbabu, A. P.; Dogra, N.; Dhara, S. 2, 5-Dimethoxy 2, 5-Dihydrofuran Crosslinked Chitosan Fibers Enhance Bone Regeneration in Rabbit Femur Defects. *RSC Adv.* **2014**, *4*, 19516−19524.
(47) Frisch, M. J.; Trucks, G. W.; Schlegel, H. B.; Scuseria, G. E.; Robb, M. A.; Cheeseman, J. R.; Scalmani, G.; Barone, V.; Mennucci, B.; Petersson, G. A.; Nakatsuji, H.; Caricato, M.; Li, X.; Hratchian, H. P.; Izmaylov, A. F.; Bloino, J.; Zheng, G.; Sonnenberg, J. L.; Hada, M.; Ehara, M.; Toyota, K.; Fukuda, R.; Hasegawa, J.; Ishida, M.; Nakajima, T.; Honda, Y.; Kitao, O.; Nakai, H.; Vreven, T.; Montgomery, J. A., Jr.; Peralta, J. E.; Ogliaro, F.; Bearpark, M.; Heyd, J. J.; Brothers, E.; Kudin, K. N.; Staroverov, V. N.; Kobayashi, R.; Normand, J.; Raghavachari, K.; Rendell, A.; Burant, J. C.; Iyengar, S. S.; Tomasi, J.; Cossi, M.; Rega, N.; Millam, J. M.; Klene, M.; Knox, J. E.; Cross, J. B.; Bakken, V.; Adamo, C.; Jaramillo, J.; Gomperts, R.; Stratmann, R. E.; Yazyev, O.; Austin, A. J.; Cammi, R.; Pomelli, C.; Ochterski, J. W.; Martin, R. L.; Morokuma, K.; Zakrzewski, V. G.; Voth, G. A.; Salvador, P.; Dannenberg, J. J.; Dapprich, S.; Daniels, A. D.; Farkas, O.; Foresman, J. B.; Ortiz, J. V.; Cioslowski, J.; Fox, D. J. *Gaussian 09*, revision D.01; Gaussian, Inc.: Wallingford, CT, 2009.
(48) Dennington, R. D., II; Keith, T. A.; Millam, J. M. *GaussView 5.0*; Gaussian, Inc.: Wallingford, CT, 2009.
(49) Becke, A. D. Density-Functional Thermochemistry III. The Role of Exact Exchange. *J. Chem. Phys.* **1993**, *98*, 5648−5652.
(50) Lee, C.; Yang, W.; Parr, R. G. Development of the Colle-Salvetti Correlation-Energy Formula into a Functional of the Electron Density. *Phys. Rev. B* **1988**, *37*, 785−789.
(51) Becke, B. D. Density-Functional Exchange-Energy Approximation with Correct Asymptotic Behavior. *Phys. Rev. B* **1988**, *38*, 3098−3100.
(52) Lu, Y.; Li, H.; Zhu, X.; Zhu, W.; Liu, H. How Does Halogen Bonding Behave in Solution: A Theoretical Study Using Implicit Solvation Model. *J. Phys. Chem. A* **2011**, *115*, 4467−4475.
(53) Lu, Y.; Li, H.; Zhu, X.; Liu, H.; Zhu, W. Recognition of Anions Through the Combination of Halogen and Hydrogen Bonding: A Theoretical Study. *Comput. Theor. Chem.* **2012**, *980*, 138−143.
(54) Sahoo, B. K.; Mukherjee, J.; Pal, T. K. Development and Validation of a High-Performance Liquid Chromatographic Method for Bioanalytical Application with Ranitidine HCl. *Int. J. Pharm. Pharm. Sci.* **2011**, *3*, 34−38.
(55) Jinu, I.; Kaity, S.; Ganguly, S.; Ghosh, A. Microwave-Induced Solid Dispersion Technology to Improve Bioavailability of Glipizide. *J. Pharm. Pharmacol.* **2013**, *65*, 219−229.
(56) Arunbabu, D.; Shahsavan, H.; Zhang, W.; Zhao, B. Poly (AAc-co-MBA) Hydrogel Films: Adhesive and Mechanical Properties in Aqueous Medium. *J. Phys. Chem. B* **2013**, *117*, 441−449.
(57) Bardajee, G. R.; Pourjavadi, A.; Soleyman, R. Trigonal Pyramidal $CuInSe_2$ Nanocrystals Derived by a New Method for Photovoltaic Applications. *Colloids Surf., A* **2011**, *392*, 16−24.
(58) Peppas, N. A. Analysis of Fickian and Non-Fickian Drug Release from Polymers. *Pharm. Acta Helv.* **1985**, *60*, 110−111.
(59) Ritger, P. L.; Peppas, N. A. A Simple Equation for Description of Solute Release. I. Fickian and Non-Fickian Release from Non-Swellable Devices in the Form of Slabs, Spheres, Cylinders or Discs. *J. Controlled Release* **1987**, *5*, 23−36.
(60) Korsemeyer, R. W.; Gurny, R.; Doelker, E.; Buri, P.; Peppas, N. A. Mechanisms of Solute Release From Porous Hydrophilic Polymers. *Int. J. Pharm.* **1983**, *15*, 25−35.
(61) Higuchi, T. Rate of Release of Medicaments from Ointment Bases Containing Drugs in Suspension. *J. Pharm. Sci.* **1961**, *50*, 874−875.
(62) Hixson, A. W.; Crowell, J. W. Dependence of Reaction Velocity upon Surface and Agitation. *Ind. Eng. Chem.* **1931**, *23*, 923−931.
(63) Kopcha, M.; Lordi, N. G.; Toja, K. Evaluation of Release from Selected Thermo Softening Vehicles. *J. Pharm. Pharmacol.* **1991**, *43*, 382−387.

DOI: 10.1021/acsami.5b02975
ACS Appl. Mater. Interfaces 2015, 7, 14338−14351